31st International Symposium on Remote Sensing of Environment,
June 20-24, 2005, Saint Petersburg, Russian Federation

Estimating erosion in an Andean catchment combining coarse and fine spatial resolution satellite imagery

C. Saavedra [a,], C. M. Mannaerts [a]*

[a] International Institute for Geoinformation Sciences and Earth Observation, Department of Water Resources, Enschede, PO Box 6, 7500 AA, The Netherlands (saavedra@itc.nl, mannaerts@itc.nl)

Abstract – **This paper discusses results of application of five erosion models with low input data requirements to a semi-arid mountainous catchment in the Bolivian Andes. Input data for land cover was derived from SPOT-5 and MODIS-NDVI time series imagery. Topography was derived from SRTM data and soil and precipitation data were obtained locally. Model performance was evaluated in a semi-quantitative manner by overlaying the predicted spatial patterns obtained by the models with an erosion intensity map derived from comparison of an ortho-photo mosaic (1961) with a recent (2002) ortho-rectified SPOT-5 panchromatic image. Results show that three models performed reasonably well in terms of erosion intensity and soil loss redistribution. It is concluded that a relatively simple but appropriate model formulation in combination with geo information techniques and ground control may be sufficient to allow erosion assessment in ungauged catchments.**

Keywords: Remote sensing, GIS, erosion modeling, DEM, Andes, vegetation dynamics, model validation.

1. INTRODUCTION

The problem of land degradation by water erosion and sedimentation is particularly evident in the Bolivian Andes given the combination of medium textured soils, lithology, steep relief, seasonally concentrated rainfall and abandonment of agriculture. As a consequence, there is a need for a better quantitative estimation of erosion processes on these landscapes for both on-site and off-site assessment of its impact. In the last 60 years models have been built (empirical, conceptual or physically based) in order to represent and to quantify the process of detachment transport and deposition of eroded soil with the aim of implementing assessment tools for either scientific or planning purposes. Physically based models are powerful modern tools to support such understanding however, both high data demand and the paucity of high resolution data in Andean mountains catchments hamper their application. The use of remote sensing and geographic information system techniques in combination with low data demanding model makes soil erosion estimation and its spatial distribution feasible with reasonable costs and better accuracy in larger scales. For example Dwivedi et al., (1997) derived the erosion risk by classifying satellite image according to the percentage of bare soil. Mathieu et al. (1997) and Haboudane et al.(2002) improved on this scheme by estimating vegetation cover from Landsat TM and SPOT-4 data and combining them with slope generated from a DEM to produce erosion rate maps. A comparison of methods for producing maps of vegetation related variables for soil erosion studies using coarse and medium satellite imagery were applied by de Leprieur et al., (2000) and Symeonakis and Drake (2004), who founded that NDVI was the most useful. Therefore, this research explores the implementation of five erosion models based on the integration of remote sensing and GIS in a medium-sized Andean catchment. The aim of this paper was to evaluate the performance of low data demanding models in a semi-arid mountainous environment and to assess the spatial distribution accuracy of the model outputs using mapped erosion features extracted from high resolution satellite data.

2. MATERIAL AND METHODS

2.1 Brief model description

The RUSLE (Renard et al., 1997) equation has the following form:

$$E_{(r)} = R \times K \times LS_{(r)} \times C \times P \quad (1)$$

where $E_{(r)}$ [ton ha^{-1}] is the average soil loss, R [MJ mm ha^{-1}hr^{-1}] is the rainfall intensity factor, K [ton ha^{-1} per unit R] is the soil erodibility factor, $LS_{(r)}$ [dimensionless] is the topographic (length-slope) factor, C [dimensionless] is the land cover factor and P [dimensionless] is the soil conservation or prevention practices factor. To incorporate the impact of flow convergence Mitasova et al., (1996) replaced the slope-length factor ($L \times S$) by the upslope contributing area per unit of contour width $A_{(r)}$ in RUSLE-3D. The modified $LS_{(r)}$ factor at a point on a hillslope reads:

$$LS_{(r)} = (m+1)\left[\frac{A_{(r)}}{22.13}\right]^m \times \left[\frac{\sin\beta_{(r)}}{0.09}\right]^n \quad (2)$$

where $\beta_{(r)}$ is the steepest slope angle, $r_{(x,y)}$, m and n are parameters depending on the type of flow. The $LS_{(r)}$ factor accommodates irregular slopes by incorporating the amount of hillslope convexity and concavity however the effect of runoff is not fully taken into account. The Unit Stream Power Erosion Deposition model or USPED overcome this shortcoming by using a dimensionless index of sediment transport capacity $T_{(r)}$, and a topographic index E_d, representing the change in transport capacity in flow direction, to estimate the spatial distribution of both erosion and deposition. E_d is positive for areas with topographic potential for deposition and negative for areas with erosion potential. $T_{(r)}$ can be estimated as:

$$T_{(r)} = R \times K \times C \times P \times A_{(r)}^m \times (\sin\beta)^n \quad (3)$$

Corresponding author. Tel.:+31 53 4874547; fax +31 53 4874336
E-mail address: saavedra@itc.nl (Carlos Saavedra)

E_d is estimated as a change in sediment flow rate expressed by a divergence in sediment flow:

$$E_d = div(T_{(c)} \times s) = \frac{\partial(T_{(c)} \times \cos a)}{\partial x} + \frac{\partial(T_{(c)} \times sena)}{\partial y} \quad (4)$$

where a [deg] is the aspect of the elevation surface.

Morgan *et al.* (1984) developed a method to predict annual soil loss from field sized areas on hillslopes. The Modified Morgan, Morgan and Finney or MMMF includes changes to the way soil particle detachment by raindrop is simulated. It incorporates a routing algorithm and enables the input from satellite images and DEM data (de Jong et al., 1999). The distributed transport capacity map DT_c is estimated by:

$$DT_c = [Q_{cum} - K_s] \times \sin(S) \times CH \quad (5)$$

where, Q_{cum} is the potential cumulative runoff, K_s is the saturated hydraulic conductivity, S is the slope steepness and CH is a map that masks out the hydrological channel network. The transport capacity T_c [kg m^{-2}] is computed from the DT_c, slope S and the RUSLE C factor that accounts for effects of vegetation cover and soil tillage.

$$T_c = 0.001 \times C \times DT_c^2 \times Sin(S) \quad (6)$$

Soil detachment by rainfall F [kg m^{-2}] is based upon empirical relationships between rainfall energy E, soil detachability index K [kg kJ^{-1}] and percentage of rainfall interception by vegetative cover P.

$$F = 0.001 \times K[E \times \exp(0.05 \times P)] \quad (7)$$

T_c is compared with F and the lower of the two values is adopted as the annual rate of soil loss, denoting whether detachment or transport capacity was the limiting factor.

Thornes (1990) put forward a conceptual erosion model that contains a hydrological component based on a storage type analogy, a sediment transport component and a vegetation growth component. The Thornes erosion equation reads,

$$E = k \times OF^2 \times s^{1.67} \times e^{-0.07 \times v} \quad (8)$$

where, E [mm month^{-1} or mm day^{-1}] is the erosion or denudation rate depending on the time step of the model, k is a factor representing soil susceptibility to erosion and calculated from soil grain size, OF [mm per time step] is overland flow derived from hydrological sub-models of varying complexity, s [m m^{-1}] is the slope gradient and v [%] is the fraction of cover vegetation.

The stream power law model or SPL states that erosion is proportional to the product of river slope and discharge. The stream power incision model (Stock and Montgomery, 1999) can be written as:

$$E = K \times A^m \times S^n \quad (9)$$

where, E [m yr^{-1} per area unit] denotes erosion or denudation rate, K [m^x yr^{-1}] is the erosion coefficient encompassing the effects of lithology, soil and climate, A [km^2] is the upstream drainage area. S [m m^{-1}] is the slope gradient, representing the energy gradient for the erosion and denudation processes

2.2 Study area

The study area is located at 5 km from Tarata, and 35 km southeast from Cochabamba. The catchment covers an area of 59.8 km^2 (Figure 1). According to Saavedra (2000) the lithology of the Laka-Laka reservoir catchment presents a succession of Ordovician sedimentary rocks and Quaternary surficial deposits (fluvio-lacustrine, colluvial and alluvial). These are composed of pebble, gravel, sand silty and clay. The catchment has an elevation ranging from 2,700 to 3,700 masl, with slopes averaging 45 %. Two main rivers drain into the Laka-Laka reservoir and maintain a relatively important rate of flow during the rainy months and become intermittent during the dry season. During summer months (December to March), 80 % of annual precipitation is recorded, the average annual rainfall being in the range of 504 mm yr^{-1}.

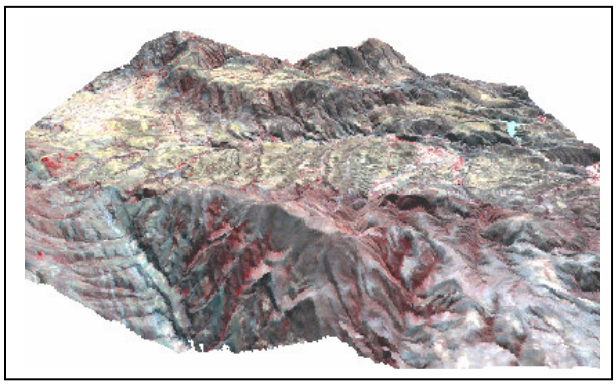

Figure 1. SPOT-5 False colour composite 3D image of the catchment

2.3 Data preparation

SPOT-5 taken on July 2002 was ortho-rectified with 90 ground control points and a 30 m DEM data using ERDAS 8.7 Ortho-Base with a root mean square error RMSE of less than 0.89 pixels. 1:50,000 aerial photographs taken on August 1961 were ortho-rectified based on the SPOT-5 corrected image, and a photo-mosaic with 5 m spatial resolution was derived. During the field data survey conducted in August 2003, 65 ground truth georeference points were collected for supervised land cover classification. The maximum likelihood classifier (MLC) was used. The NDVI from SPOT-5 was used to calculate the factor C considering that NDVI was highly correlated with vegetative cover and biomass. Calibration values of C for the individual sample plots were determined using RUSLE 1.6 software and field data. A linear regression was computed between the NDVI values and the corresponding C values from the field. The temporal variation of vegetation cover [%] across the catchment was estimated using the 16-day time series MODIS-NDVI imagery using the regression relationship of Zhang (1999).

A soil map was generated based on the interpretation of pedoforms and landforms using the 1961 ortho-photo. 18 representative soil profile samples were collected, described and characterized according to the Soil Survey Staff (1993).

Contour lines, rivers and typical points were digitized based on 1:50000 topographic maps and were used to generate the 30 m DEM and to assess the usability of the 90 m SRTM DEM data for catchment erosion assessment. To select the proper upslope contributing area A_r, we compared results obtained with the *D8*, multiple and combined flow algorithms available in TAUDEM (Tarboton, 2004). Careful visualization assessment of each map using an overlay of catchment tributaries resulted in the selection of the multiple flow algorithm due to its close approximation of the existing stream networks. The monthly overland flow OF_i [mm] generation algorithms proposed by Zhang (1999) were used, and read as:

$$OF_i = \int_{I_a}^{\infty} OF_p \times J_i \times \Delta r \qquad (10)$$

where OF_p is the overland flow in a rainfall event, J_i is the rain day frequency density function and Δr is the increment of rainfall per rain day.

An actual erosion feature map was derived by combining information from a field reconnaissance erosion survey where the more important erosion features were georeferenced, a supervised classification of these features using SPOT-5 and a delineated feature map of these patterns from the ortho-photo mosaic, so that the maximum level of accuracy of the model predictions could be verified.

3. DISCUSSION AND RESULTS

The modeled soil loss values obtained with the five models were grouped into five ordinal intensity classes using a frequency distribution analysis, resulting in erosion maps as the displayed on Figure 2. From the model output predictions (Table A) it was found that on average, 2.1×10^5 tonnes of soil are moved annually and the average erosion rate predicted is 42.7 ton ha^{-1} yr^{-1}. We evaluated that in general terms 20 % of the catchment experiences slight erosion whereas 50.7 % of the area is considered moderate. The proportion of area with high and severe intensity of erosion is 23.5 and 5.8 % respectively. Overall 29.3 % of the area is undergoing high erosion rates which are the major contributors to sediment yield in the catchment. Analysis of the results shows that the highest values are predicted by the RUSLE-3D, because it gives more importance to both the topographic forcing in steep areas generating large values of $LS_{(r)}$ and the rainfall erosivity factor R. In addition, USPED estimates areas where deposition occurs. Both models include the impact of sheet and rill flow on hillslopes as well as concentrated flow erosion and potential for gully formation hence, it may not be necessary to add the impact of gullies as observed in the field because they are already incorporated. MMMF and SPL model predict lower values of erosion. According to these models an average of 48.8 and 63.7 % of the area present slight erosion rates respectively.

Table A. Area [%] of erosion intensity classes

Rate of erosion	Rusle-3D	MMMF	SPL	Thornes	USPED
ton ha^{-1} yr^{-1}	Area [%]	Area [%]	Area [%]	Area [%]	Area [%]
0 - 2	10.9	37.3	21.8	20.0	10.0
2-8	15.7	11.5	43.7	14.6	12.5
8-32	24.9	34.0	30.6	22.7	44.0
32 - 128	40.0	17.2	3.7	26.0	11.0
> 128	8.5	0.0	0.2	16.6	0.1
deposition					22.5
Total	100	100	100	100	100

The Thornes model predicts slight and moderate values of erosion for areas between 1 to 40 % of slope gradient. It estimates that 43.3 % of the catchment is exposed to high to severe rates of soil losses however, within this category there are areas with slopes greater than 60 % (5.9 km^2) which are not experiencing high soil losses. This erroneous prediction can be explained by the effect of the runoff and slope. Runoff is designed to use average daily rainfall, and by not considering a rainfall intensity distribution, we may be masking the short periods of intense rainfall that generate brief Hortonian overland flow.

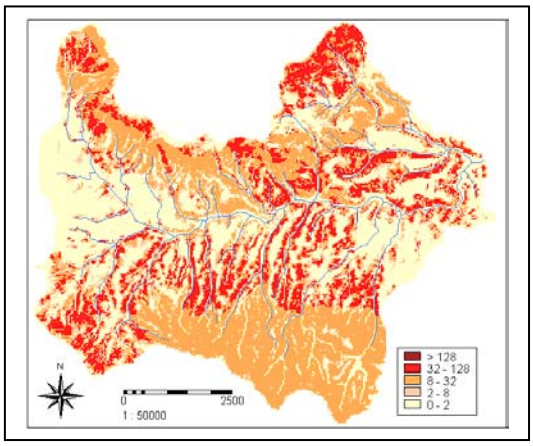

Figure 2. Predicted erosion rates using MMMF

Table B. Mapping validation using an erosion feature map

ID	RUSLE-3D	MMMF	SPL	Thornes	USPED
	MA [%]	MA [%]	MA [%]	MA [%]	MA [%]
a	45.2	55.2	48.9	30.8	38.0
b	41.8	47.7	46.1	44.7	42.8
c	40.3	46.3	23.1	53.2	52.3
d	42.8	35.6	35.6	38.5	44.2
e	50.0	60.0	30.0	16.5	40.0
f	44.2	37.9	40.4	31.6	36.6
g	34.0	34.0	36.3	40.8	22.7
WA	42.8	47.1	42.0	42.7	43.6

[MA] mapping accuracy, [a] slight interrill and rill erosion, [b] moderate interrill and erosion, [c] severe interrill and rill erosion, [d] slight active gullies, [e] moderate active gullies, [f] severe active gullies, [g] channel erosion and [WA] weighted accuracy.

Due to the paucity of validation data in the researched catchment, the overall reliability of the models was validated using a semi-quantitative technique. The predicted maps were compared with the erosion feature map hence, the overall mapping accuracy of each erosion intensity class was estimated (Table B). The model results are in agreement with the locations of existing severe erosional features (*e.g.,* ephemeral gullies, active gullies and bank erosion) in particular when MMMF and RUSLE-3D models are considered. The validation indicates that areas classified as slight, moderate and severe rill/interrill erosion in the feature map are correctly predicted with an average of 43, 44 and 44 % by all models, respectively. The mapping accuracy reduces to an average of 38, 39, 39 and 33 % in the case of prediction

for areas classified as slight, high, severe active gully erosion and channel erosion

These fair prediction rates can be related to five factors: *(1)* the low response of vegetation to rainfall, *(2)* the gradual intensification of rainfall intensity as the wet season progresses, *(3)* intense rainfall events in steep mountains have a high runoff that induces a major potential for transport capacity of the eroded soil, *(4)* overland flow affects the energy triggering soil erosion especially after the end of the dry season and *(5)* the non linear relationship between vegetation cover and erosion means that erosion is very high in bare areas, but lowers rapidly when the fraction of cover vegetation increases.

4. CONCLUSIONS

In this paper, the ability to predict erosion based on satellite imagery parameters in combination with models such as USPED, RUSLE-3D, SPL and MMMF have been illustrated. These models try to capture the essence of reality using only topographical parameters, and basic thematic data to represent the variety of soil loss redistribution processes. When simulating erosion at seasonal time scale we believe that these kinds of approaches are more appropriate than sophisticated physically based erosion models (*e.g.,* WEPP, EUROSEM).

The integration of the topographic, meteorological, field surveyed and remotely sensed data, within a GIS provides an environment for effective evaluation of various modeling approaches to erosion deposition assessment at catchment scale. The high temporal resolution MODIS-NDVI time series images in combination with SPOT-5 proved to be valuable data for both continuous monitoring of the vegetation dynamics and derivation of vegetation parameters required for the different soil erosion models.

When paucity of erosion measurements exists model calibration and validation are hampered, remote sensing imagery provides a spatially explicit background for indirect model validation. The model validations demonstrated that none of the five models accurately predicts soil erosion across the catchment. It is therefore concluded that although the spatial patterns of predicted erosion by the different models seem reliable, quantitative prediction should be interpreted with caution. In terms of spatial distribution the MMMF is more appropriate for identification of sediment sources at the catchment scale (*e.g.,* high predicted erosion rates match with areas under current intense process of soil loss). RUSLE-3D and Thornes showed sufficiently reliable results and since the input data required for them are lower and easier to obtain, they are probably more suitable for predicting soil erosion in situations where detailed catchment data is not readily available.

All the implemented models are based on modest data requirements; a common limitation in Bolivia. Their practical utility is based upon providing a means for evaluating and comparing erosion factor changes among alternative land areas, besides a prediction of the absolute soil erosion for a particular location can be obtained.

5. ACKNOWLEDGEMENTS

We would like to acknowledge the Hydraulic Laboratory University of San Simon in Cochabamba (LH-UMSS) for providing technical support and ISIS (http://medias.obs-mip.fr/isis/) for providing a low cost SPOT-5 imagery. We extend special thanks to others researchers for their contribution: F. Carrrera, H. Villarroel, J. Inocente, D. Flores Cartagena, M. Ledezma, A. Coca.

6. REFERENCES

de Jong, S.M. et al., 1999. Regional assessment of soil erosion using the distributed model SEMMED and remotely sensed data. Catena, 37(3-4): 291-308.

Dwivedi, R.S., Kumar, A.B. and Tewari, K.N., 1997. The utility of multi-sensor data for mapping eroded lands. International Journal of Remote Sensing, 18(11): 2303-2318.

Haboudane, D., Bonn, F., Royer, A., Sommer, S. and Mehl, W., 2002. Land degradation and erosion risk mapping by fusion of spectrally based information and digital geomorphometric attributes. International Journal of Remote Sensing, 18: 3795-3820.

Leprieur, C., Kerry, Y.H., Mastorchio, S. and Meunier, J.C., 2000. Monitoring vegetation cover across semi-arid regions: Comparison of remote observations from various scales. International Journal of Remote Sensing, 21(2): 281-300.

Mathieu, R., King, C. and Bissonnais, Y., 1997. Contribution of multi-temporal SPOT data to the mapping of a soil erosion index. The case of the loamy plateaux of northern France. Soil Technology, 10(2): 99-110.

Mitasova, H., Hofierka, J., Zlocha, M. and Iverson, L.R., 1996. Modeling topographic potential for erosion and deposition using GIS. International Journal of Geographical Information Science, 10(5): 629-641.

Morgan, R.P.C., Morgan, D.D.V. and Finney, H.J., 1984. A predictive model for the assessment of erosion risk. Journal of Agricultural Engineering Research, 30: 245-253.

Renard, K.G., A., F.G., Weesies, G.A., McCool, D.K. and Yoder, D.C., 1997. Prediction of soil erosion by water: A guide to conservation planning with the revised universal soil loss equation (RUSLE). Agric. Handbook 703. USDA, Washington D.C.

Saavedra, C.P., 2000. Estimation of Water & Sediment Yields of watersheds using RS, GIS & Hydrologic Modelling System. A case study in the High Valleys, Cochabamba, Bolivia, International Institute for Aerospace and Earth Sciences, Enschede, The Netherlads, 120 pp.

Soil Survey Staff, 1993. Soil Survey Manual. USDA-SCS Agricultural Handbook, USDA Soil Conservation Service, Washington, D.C.

Stock, J. and Montgomery, D.R., 1999. Geologic constraints on bedrock river incision using the stream power law. Journal of Geophysical Research, 104: 4983-4993.

Symeonakis, E. and Drake, N., 2004. Monitoring desertification and land degradation over sub-Saharan Africa. International Journal of Remote Sensing, 25(3): 573-592.

Tarboton, D.G., 2004. TAUDEM. Terrain Analysis using digital elevation models. Utah State University, Logan, Utah, USA.

Thornes, J.B., 1990. Vegetation and Erosion: Processes and Environments. Wiley, Chichester.

Zhang, X., 1999. Remote sensing and GIS for modelling soil erosion at the global scale. PhD Dissertation Thesis, Kings College London, London, UK.